Cold Regions Science and Technology 170 (2020) 102954

Contents lists available at ScienceDirect

Cold Regions Science and Technology

journal homepage: www.elsevier.com/locate/coldregions

Full length articles

Oceanographic observations in supercooled water: Protocols for mitigation of measurement errors in profiling and moored sampling

N.J. Robinson[a,*], B.S. Grant[a], C.L. Stevens[a,b], C.L. Stewart[a], M.J.M. Williams[a]

[a] *Marine Physics, National Institute of Water and Atmospheric Research, Wellington, New Zealand*
[b] *Department of Physics, University of Auckland, New Zealand*

ABSTRACT

Supercooled water is liquid water that is colder than its pressure- and salinity-dependent freezing temperature. As supercooling is a metastable state, it is sensitive to small environmental changes that may force switches between solid and liquid phases, including disruption from instruments introduced to the environment. Here we present a thoroughly-tested set of observational protocols that have been developed over 15 years working in supercooled Ice Shelf Water in McMurdo Sound, Antarctica. We identify the four issues most commonly encountered in observations of supercooled ocean water as (i) the requirement for an extended process of thermal equilibration, (ii) contamination by ice within conductivity cells, (iii) anchor ice accumulation on suspended equipment, and (iv) ice coating and resultant sensing of artificially-produced latent heat. We present protocols for identifying and managing these potential modes of corruption, which include determining and allowing appropriate time for thermal equilibration, identifying and eliminating data that have been corrupted by ice capture and growth, and practical steps that can be taken to minimise accumulation of anchor ice on suspended equipment. We stress the need for planned data redundancy to enable identification and elimination of data contaminated by ice capture and phase change. We also include a complete procedure for CTD profiling which includes a 10-min soak (for an instrument initially warm relative to the ocean) and exercises data redundancy in the form of multiple up- and down-casts. Finally, we discuss how these protocols may be extended to other platforms since there is increasing scope for ice-related contamination of data as access to ice-covered oceans, and the use of autonomous vehicles in the polar oceans, increases.

1. Introduction

A supercooled fluid is one which remains liquid despite being colder than the surface freezing point ('potentially supercooled') or the in situ freezing point ('in situ supercooled'). Importantly, in situ supercooling enables the presence of suspended ice crystals, known as frazil, which can make instrumental observation problematic. Here we explore some of the issues encountered when making oceanographic measurements of in situ supercooling seawater (n.b. in the following, 'supercooling' refers to in situ supercooling unless stated otherwise).

A large body of literature exists characterising supercooling in freshwater lakes, rivers, and associated engineering infrastructure (Richard and Morse, 2008; Dubé et al., 2014; Block et al., 2019), motivated by the need to understand and overcome problems caused by accumulations of frazil ice, such as blocking intake pipes (e.g. Daly, 1991). For the marine environment, early reports of supercooling have proven controversial: Coachman & Barnes (1962), reported several instances of water supercooled by up to 80 mK in the Eurasian Basin. However, Untersteiner & Sommerfeld (1964) chose to observe supercooling implicitly, rather than require the 'hardly attainable accuracy and speed' of instruments available to them. Lewis and Perkin (1983) raised further concerns around incorrect characterisation of supercooled water owing to instrument inaccuracy and errors in the determination of the freezing point.

More recently, technological advancements in instrument capability, and improved accuracy of the freezing point determination (Fofonoff and Mallard, 1983; Feistel, 2008; McDougall and Barker, 2011), have allowed increasingly reliable characterisation of oceanic supercooling. Observed supercooling in the Arctic has primarily been derived from heat and mass exchange at the surface, yielding supercooling on the order of 1–2 mK in Freemansundet, Svalbard (McPhee et al., 2013); 7 mK in the Chucki Sea (Ito et al., 2015), 10 mK in the St Lawrence Island Polynya (Drucker et al., 2003), an estimated 20 mK in the Wandel Sea off NE Greenland (Kirillov et al., 2018); and 37 mK in Storfjorden, Svalbard (Skogseth et al., 2009). Notably, in all of these observations the duration of the appearance of supercooling at the measurement point has been brief (minutes to hours). In addition, Morozov et al. (2015) reported supercooling of 350 mK associated with the glacial discharge of the Paula Glacier.

In the Antarctic, pressure-driven supercooling of Ice Shelf Water (ISW) associated with ice shelf melt (Fig. 1) exported from the largest and coldest ice shelf cavities becomes prevalent. Examples of observed supercooling include ~20 mK near Filchner Ice Shelf (Foldvik and Kvinge, 1977); 35 mK beneath Ronne Ice Shelf (Nicholls et al., 2004); 6–50 mK near the Ross Ice Shelf (Smith et al., 2001; Mahoney et al., 2011; Leonard et al., 2011; Robinson et al., 2014); and 30–160 mK in front of the Amery Ice Shelf (Shi et al., 2011). Importantly, these

* Corresponding author.
E-mail address: natalie.robinson@niwa.co.nz (N.J. Robinson).

https://doi.org/10.1016/j.coldregions.2019.102954
Received 23 October 2018; Received in revised form 28 October 2019; Accepted 18 November 2019
Available online 20 November 2019

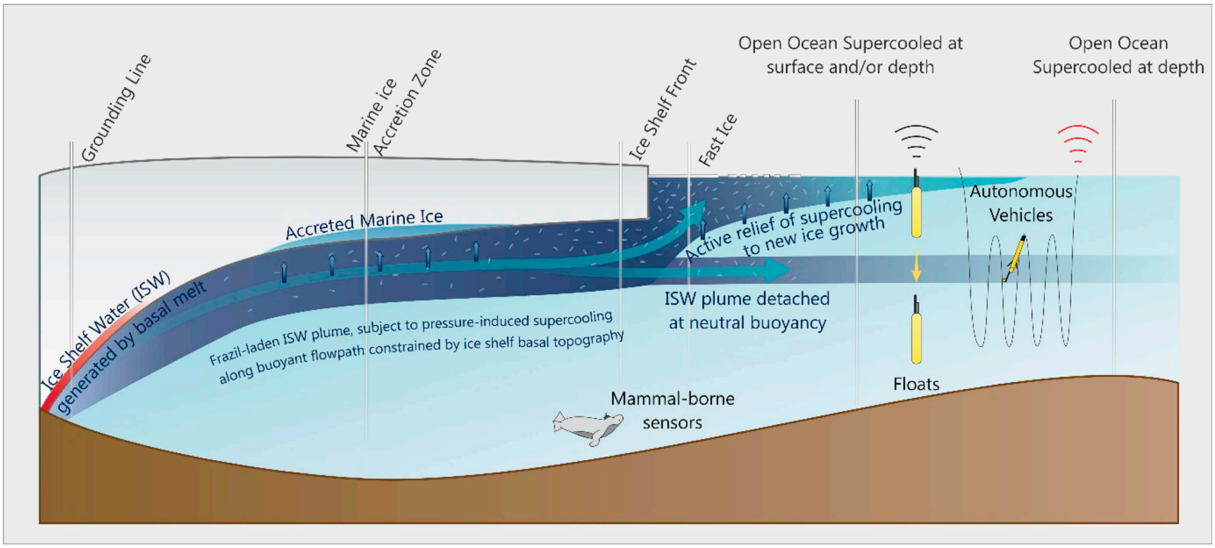

Fig. 1. Schematic showing the formation and buoyant flow of supercooled Ice Shelf Water (ISW). The potentially-affected zones range from the ice shelf grounding line to the open ocean. The issues described herein have potential applicability to a range of possible observational platforms including traditional profiling and moored deployments, mammal-borne instrumentation and autonomous floats and vehicles. The present study region is represented by the fast ice immediately adjacent to the front of the ice shelf and is characterised by a deep and sustained supercooled ISW plume, which is laden with frazil ice crystals in suspension, and which supports the development of thick, unconsolidated platelet layers at the base of the sea ice.

pressure-driven conditions persist for days if not months (Dempsey et al., 2010), heightening the potential for capturing unreliable data due to ice contamination of sensors (as identified by Smith et al., 2001; Robinson et al., 2014). Identifying the presence and nature of this contamination requires understanding of the dynamic and delicate balance between the degree of supercooling and growth of crystals suspended within it, as well as the possibility of disrupting this balance by the attempt to observe it.

1.1. Sources of supercooling, ice nucleation and seeding

The studies cited above provide examples of the three generations mechanisms of supercooling that have been identified for the marine environment. We describe these briefly here, but the reader is referred to Mager et al. (2013) for more complete descriptions:

(i) *Heat exchange at the air-ocean interface:* when the ocean surface is in contact with a cold atmosphere, heat exchange can lead to cooling of the upper ocean to lower than the surface freezing temperature. Mixing by convective overturning or wind stirring may extend this reach to the base of the mixed layer. Supercooling generated by this mechanism is typically a few milliKelvin (e.g. Drucker et al., 2003; Ito et al., 2015), although Skogseth et al., (2009) observed supercooling of 37 mK produced by this method and sustained for ~ 2 min.

(ii) *Heat exchange between water masses of different salinity:* when two water masses each at their in situ freezing temperature but possessing different salinities come into contact, supercooling of the fresher water mass may occur because heat and salt diffuse between them at different rates. In the case of a sharp salinity front near the fast ice edge (McPhee et al., 2013), supercooling of 1–2 mK by this mechanism appeared on both flood and ebb phases of the tidal cycle. In contrast, exchange between fresh sub-glacial outflow and ambient ocean water at its freezing point (Morozov et al., 2015) gave rise to 350 mK of supercooling. This effect has successfully been reproduced and studied in laboratory studies by Stigebrandt (1981) and Kylov and Zatsepin (1992).

(iii) *Pressure relief of deep ice melt:*Foldvik and Kvinge (1974; 1977) identified that freshwater produced when ice is melted at depth will rise under its own relative buoyancy. In doing so it will traverse the in situ pressure-dependent freezing point to find itself colder than the new local freezing point – hence identified as 'supercooled'. This promotes the growth of frazil crystals which, while they remain in suspension, enhance the buoyancy of the bulk fluid leading to a 'conditional instability' (Foldvik and Kvinge, 1974). The instability is resolved when the crystals grow sufficiently large that their buoyancy overcomes suspension by turbulence and they are gravitationally removed from the system (to gather at the ocean surface or accrete at a solid ice-ocean interface). A few instances of pressure-induced supercooling from melting of sea ice keels (e.g. 8 mK of supercooling observed by Lewis and Perkin, 1983) and marine-terminating glaciers (e.g. Tweed et al., 2005) have been noted for the Arctic. However, more substantial supercooling is generated by melting of floating ice shelves in the Antarctic, as identified above.

Regardless of its mechanism of generation, supercooling in the ocean supports suspension and growth of frazil ice crystals. The observation of rapid growth of suspended frazil ice, accompanied by the release of latent heat which relieves the supercooling (e.g. Carstens, 1966), has led some researchers to the conclusion that supercooling is an inherently unstable state which cannot persist for a long time (e.g. Lewis and Lake, 1971; Morozov et al., 2015). However, this treatment is not borne out by observation (e.g. Muller, 1978) or theory (see below), and instead leads to the conclusion that supercooling of < 1 K in the marine environment is a metastable state (Büchner and Heuer, 2000) which can persist indefinitely in the absence of suitable sites for crystal growth (Dorsery, 1948; Daly, 1984).

Central to the discussion of supercooling longevity and potential for ice contamination of observations is the process of nucleation, which is necessary for relief of supercooling through ice growth. Daly (1984) reviewed the mechanics of nucleation and identified pathways as homogeneous primary, heterogeneous primary and secondary nucleation: Pure water must be cooled to -38 °C in order to promote spontaneous homogenous primary nucleation. The addition of foreign particles suspended in the liquid provides sites for heterogeneous nucleation, although nucleation doesn't appear for supercooling < 1 K (Hobbs, 1974; Daly, 1984). Secondary nucleation or 'collision breeding' is the most common pathway for crystal creation via multiplication of suspended ice crystals present in the liquid through collisions with hard

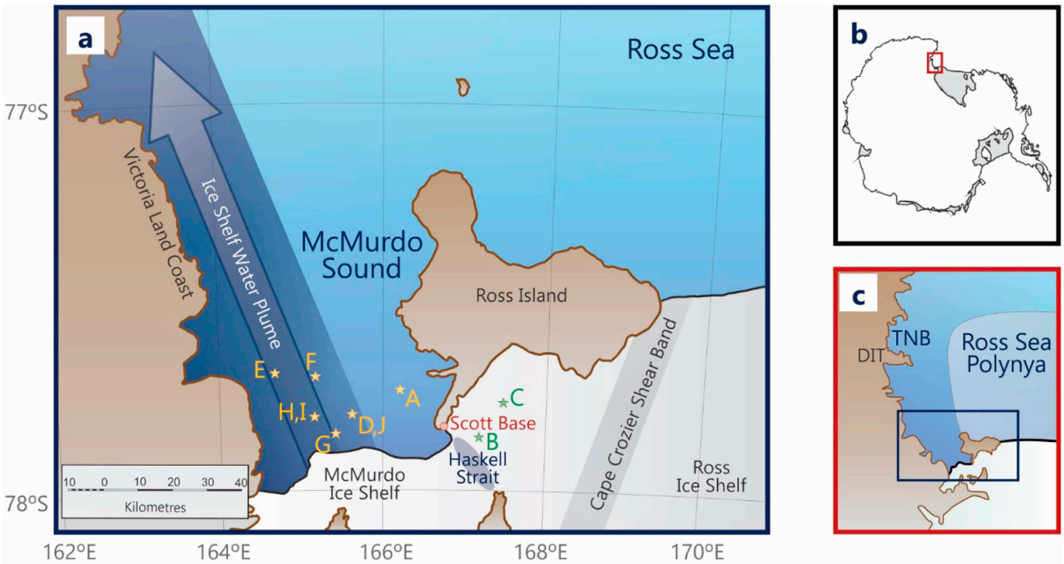

Fig. 2. a: Map of McMurdo Sound identifying the locations of the ten field campaigns (Yellow = sea ice sites, Green = ice shelf sites) and the geophysical features referred to in the text. Coloured borders (a, b, c) indicate the geographical context of the study region.

surfaces (including each other) or fluid shear (Daly, 1984; Wang and Doering, 2005; Rees Jones and Wells, 2018).

It is clear that the presence of supercooled water and any associated frazil crystals is highly sensitive to environmental variations that could force a switch in local conditions relative to the in-situ freezing point. Processes such as pressure changes from internal wave propagation (Robinson, 2012); injection of brine into the surface water during the sea ice growth process (Lewis and Lake, 1971; Skogseth et al., 2009); or addition of latent heat during ice formation can drive a change of supercooling state or phase (i.e. from liquid to solid or vice versa). In a similar manner, instruments and equipment introduced to supercooled water could disrupt the delicate balance in the immediate vicinity of the sensors (e.g. Skogseth et al., 2009; McPhee et al., 2013), leading to incorrect measurement and erroneous characterisation of the natural state.

Supercooled ISW is being observed in a growing number of locations in the Antarctic (Dieckmann et al., 1986; Engelhardt and Determann, 1987; Grosfeld et al., 1998; Fricker et al., 2001; Holland et al., 2009; Shi et al., 2011; Hattermann et al., 2012; Langhorne et al., 2015; Hoppmann et al., 2015), and the true spread of supercooled ISW is likely to be much wider in the coastal Antarctic ocean (see for example Kusahara and Hasumi, 2014). McMurdo Sound is one of the key Antarctic locations for crystal growth in supercooled water, with observations dating back to the British National Antarctic Expeditions (Hodgson, 1907) and on multiple occasions since (e.g. Wright and Priestley, 1922; Littlepage, 1965; Dayton et al., 1969; Lewis and Perkin, 1985; Langhorne et al., 2015)

Since 2002 the authors of the present study have, alongside colleagues, conducted 25 field campaigns in this region aimed at understanding the export of ISW from the Ross Ice Shelf cavity, and so have encountered supercooled water in a variety of settings and conditions. On several occasions it has become apparent that portions of the oceanographic data were corrupted as a result of instrument response to suspension in supercooled water. This experience has motivated the development of pre- and post-deployment techniques for instrument preparation and treatment of data, with the aim of retaining high quality, reliable information suitable for characterising this unique water mass.

In the following sections, we document the presence and impacts of supercooling during these campaigns and identify the four most-frequently encountered issues: thermal equilibration, contamination by ice within the conductivity cell, anchor ice on suspended equipment, and ice coating of sensors. We discuss recommended solutions to these issues and extend this experience to the newer generation of sampling platforms.

2. Methods

2.1. Oceanographic setting

McMurdo Sound is located at the north-western corner of the Ross Ice Shelf. A stable and consistent supply of ISW, originating with melt of the Ross Ice Shelf, flows through Western McMurdo Sound where it takes the form of an ISW plume ~170 m thick and up to 30 km wide. Owing to relief of pressure along its flow path immediately prior to entering the Sound, the plume is supercooled over the upper ~70 m, by as much as 50 mK at the ice-ocean interface (Fig. 1; Robinson et al., 2014). This flow supports the inclusion of platelet crystals in the consolidated sea ice cover (Dempsey et al., 2010; Hughes et al., 2014) and a widely distributed sub-ice platelet layer (Langhorne et al., 2015). Elsewhere in the sound, intrusion of ISW is pervasive but not as deep or consistent (e.g. Smith et al., 2001; Leonard et al., 2011; Mahoney et al., 2011).

Here, illustrative examples of data, representing a combination of both moored and profiling sampling strategies, are taken from eight separate observational experiments on McMurdo Sound fast ice and two experiments on the McMurdo Ice Shelf over a 15-year period between 2003 and 2017 (See Figs. 2 and 3, and Table 1). At all ten sites, platelet ice was reported in some form beneath the solid ice cover. At the ice shelf sites this was limited to a few small crystals in suspension near the ice base (Barrett et al., 2005; Robinson et al., 2010). However, for all sea ice sites reported here, the crystals formed a semi-rigid, unconsolidated platelet layer immediately adjacent to the sea ice base.

Such layers are tangible evidence of strong ice shelf influence, as they can only develop and be maintained if supported by flow of supercooled ISW. Sub-ice platelet layers up to 9 m thick have been observed beneath first-year sea ice by the authors within the main ISW flow and near the ice shelf front. In such cases, preparing the hole ready for instrument deployment may take up to 2 h. This is typically achieved by breaking up the platelet layer with a weighted rope and then sieving out the released platelets by hand as they float up to the surface of the water. In recent seasons (2017 and 2018) we have trialled a pump capable of handling 2-phase flow, but this system is still in development.

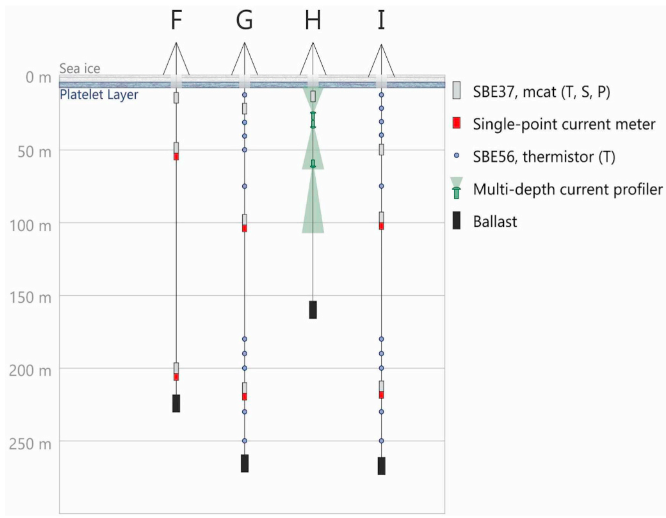

Fig. 3. Schematic diagrams of the four moored data sets (F, G, H, I) referred to in the text. See Fig. 2 for locations.

In all cases (data sets A – J, Table 1) data were collected from top-mounted instruments suspended in the ocean through holes in the ice. Data sets B & C were collected through 70 and 144 m of ice shelf, with access gained via Hot Water Drilling. For the remaining data sets (A; D – J) access to the sub-sea ice ocean was gained via an ice auger that generated a 10″ (25 cm) hole. Moored instruments (Fig. 3) were suspended from a tripod mounted over the access hole, and an electric winch was used for profiling instruments. Details of instruments used in each deployment are given in Table 1, and manufacturer's specifications for accuracy and precision of each instrument type are shown in the Appendix.

2.2. Use of TEOS-10

Observations and findings are reported here using the Gibbs function for seawater thermodynamics (Feistel, 2008), applying the scripts generated by McDougall and Barker (2011), and using the latest version of the toolbox available at the time of writing (http://www.teos-10.org/software.htm). To our knowledge, no measurements of the ion ratio (which is a significant point of difference from the UNESCO formulation; Fofonoff and Mallard, 1983) have been made for Antarctic Ice Shelf Water. As this water mass is defined by inclusion of glacial melt, this deficiency could introduce a source of uncertainty for this application. However, the difference in calculated supercooling between the formulations is < 1 mK, as was also found by Ito et al. (2015), and hence does not emerge above the level of observational uncertainty.

2.3. Terminology

In the present study, observed temperatures will be presented in °C, but translations to degrees of supercooling will be presented in K, as is the convention emerging in the literature (e.g. Smith et al., 2001; Skogseth et al., 2009; McPhee et al., 2013).

Supercooled water supports a number of ice forms. In this work we apply the following definitions:

(i) Ice seeds: suspended ice crystals that are able to act as nucleation for further ice growth. Ice seeds may be too small to be visible to the naked eye, especially under field conditions.
(ii) Frazil ice: Ice crystals that are large enough to be visible yet small enough to remain in suspension by turbulence.
(iii) Ice Platelets: Large individual crystals or 'plates' of ice that initiated as suspended frazil but have undergone sufficient growth to become buoyant and rise out of the water column. Where they are trapped by sea ice cover at the surface, they may loosely accumulate to form a 'sub-ice platelet layer' or become incorporated into the consolidated sea ice cover.
(iv) Anchor ice: Following Daly (1984) and Mager et al. (2013) we define anchor ice as 'submerged ice attached to a substrate, for example the bed of a river, lake, or sea'. We follow Reimnitz et al. (1987) and extend this definition to accumulations of ice on ropes, instruments and other equipment suspended in the supercooled flow.

3. Results: issues and management

In this section, we describe the four most common issues associated with deployments into supercooled ocean water, listed in the order that they are likely to be encountered in a specific deployment. We offer practical solutions or management criteria for each of the issues that have been developed over 15 years of field work and experimentation in supercooled waters in McMurdo Sound. The order in which the issues are presented does not suggest a 'hierarchy' of corruption, and all modes should be considered simultaneously in the situations for which they are relevant.

Table 1
Summary of the ten field campaigns referenced in the text. See Fig. 2 for locations.

Ref	Date(s)	Data type	Instruments	Latitude	Longitude	Depths surveyed (m)	Potential temperature (°C)	Salinity (PSU)	Max flow speed (cm/s)
A	9–11 Nov 2004	99 Profiles	SBE19plus	77.7581°S	166.0819°E	0–250	−1.93 to −1.91	34.62–34.71	30
B	15 Jan 2003	13 Profiles	SBE37-SM	77.8885°S	167.0844°E	0–900	−1.95 to −1.25	32.80–34.80	25
C	29 Jan 2003	10 Profiles	SBE37-SM	77.8352°S	167.3368°E	0–800	−1.93 to −1.88	34.40–34.80	20
D	13 Nov 2016	Profile	SBE19plus	77.7659°S	165.6037°E	0–500	−1.96 to −1.91	34.50–34.70	30
E	11 Nov 2016	Profile	SBE19plus	77.6667°S	164.7994°E	0–150	−1.94 to −1.92	34.63–34.65	Unknown
F	9 Nov – 5 Dec 2007	Mooring	3x SBE37 2x RCM	77.6662°S	165.1115°E	15, 50, 200	−1.96 to −1.91	34.65–34.74	20
G	31 Oct – 13 Nov 2016	Mooring	4x SBE37 2x RCM 10x SBE56	77.8183°S	165.4059°E	10, 20, 30, 40, 50, 75, 100, 180, 190, 200, 210, 230, 250	−1.97 to −1.91	34.62–34.69	30
H	3–6 Nov 2017	Mooring	Sn1000 2x Sn500 2x Nobska SBE37	77.7667°S	165.2°E	10–120	−1.96 to −1.91	34.60–34.65	20
I	3–21 Nov 2017	Mooring	3x SBE37 2x seaguard 10x SBE56	77.7667°S	165.2°E	10, 20, 30, 40, 50, 75, 100, 180, 190, 200, 210, 230, 250	−1.96 to −1.91	34.61–34.68	35
J	18 Nov 2017	Profile	SBE19plus	77.7667°S	165.2°E	0–300	−1.96 to −1.93	34.6–34.66	20

3.1. Thermal equilibration

Thermal equilibration refers to the process by which the thermal differential between an instrument and the ocean into which it is deployed is reduced over time. While equilibration requires time to proceed at any location (Pawlowicz, 2013), the observed supercooling has been characterised within just two orders of magnitude of the stated accuracy of the instruments. This requires that the equilibration is complete to a degree that corresponds with instrument resolution and natural variation in the water column – that is, there is far less tolerance for residual thermal lag than would be permissible in temperate waters.

The thermal differential when the instrument is initially colder than the ocean may be substantial and is likely to be accompanied by corruption by other mechanisms. If, for example, an instrument has been transported or stored at very cold temperatures, by the time of deployment its temperature may be many degrees colder than the freezing point of the ocean. Deployment into water that is near or below its own freezing temperature will therefore promote rapid ice formation onto the instrument. Such ice growth may be initiated by adhesion of suspended ice seeds (Reimnitz et al., 1987; Daly, 2008), or the instrument may be so cold that it cools the water surrounding it sufficiently (i.e. to > 1 K supercooled) that primary heterogeneous nucleation is initiated. As long as the instrument remains suspended in supercooled water this situation is not recoverable, since there is no opportunity for this ice to melt from the instrument.

In such a situation, the initial thermal disequilibrium is likely to activate multiple further modes of data corruption (discussed below) including depth change if icing becomes sufficient to cause flotation, capture and growth of ice crystals within the conductivity sensor, and encasement of ice and insulation from the water being observed.

However, thermal equilibrium may still present a problem even when the instrument is initially warm relative to the supercooled water. Early in the authors' association with supercooled water, repeat hydrographic profiles were collected with a SBE19plus CTD (Conductivity-Temperature-Depth) from inside a heated shipping container (data set A collected in 2004, Fig. 3, Table 1; reported by Albrecht et al., 2006). At the beginning of each individual cast, the CTD was suspended in the surface water that, because it was relatively fresh, was buoyantly trapped at the top within the sea ice hole. This surface water had warmed to approximately +0.5 °C through contact with the warm environment of the shipping container. Thus, the thermal differential with the supercooled water beyond the base of the sea ice was reduced to < 2.5 °C by the time intentional data collection commenced.

According to the recommendation of the instrument manufacturer for standard deployments, downcast data were used exclusively in the subsequent analysis, since, due to location of sensors, they are unaffected by the wake generated by movement of the instrument through the water column. In the original processing of these data, downcast data were not compared with upcast data, nor were the upcasts used in the published analysis.

Subsequently, we have discovered that the residual ~2.5 °C temperature difference led to an incorrect interpretation of the upper boundary layer structure. This was because the process of thermal equilibration was not sufficiently complete to achieve the high degree of accuracy required for water close to, or below, its freezing point. Downcast data consistently suggested cooling with depth, matched by a gradual salinity increase, moving smoothly into a layer homogeneous in temperature and salinity at approximately 80 m depth. However, consistent upcast data reveal that this homogeneous layer extends all the way up to the interface with the sea ice (Fig. 4). We interpret this difference as due to the slow thermal equilibration of the small residual thermal differential over the upper ~80 m of the instrument's descent, a process that is sufficiently complete as to be undetectable by the time of ascent. Through investigation of the temperature trace, it is apparent that the equilibration process, for this instrument at least, is not a linear function of time. Rather, near-complete equilibration occurs very quickly (i.e. within seconds) as a response to a large temperature difference. However, the residual equilibration (i.e. the final 30 mK) occurs very much slower (i.e. > 5 min; Fig. 3, right). This leads us to the solution of applying a soak of 10 min based on experience, as was also applied by Lewis and Perkin (1983) without quantification.

Errors in the temperature measurement fed through to corresponding errors in salinity estimates (Fig. 4, centre panel) from conductivity, since conductivity varies with temperature. The incorrect characterisation of the upper ocean boundary layer was scientifically significant in two ways:

- The difference in estimated temperature between down- and upcasts traversed the salinity and pressure-dependent freezing temperature. Due to this the boundary layer was assessed as being at or above freezing, while subsequent analysis of the upcast data shows that it was supercooled to ~20 m depth.
- In near-freezing waters, density is strongly controlled by salinity, with temperature being almost passive in its determination. Hence the stably-stratified structure of the upper ocean was subsequently revealed in upcast data to be neutral. This bears significant consequences for turbulent mixing and convective processes, particularly for the situation of buoyancy flux resulting from ice formation at the surface.

3.1.1. Recommended management of thermal equilibration

In many polar applications, thermal equilibration prior to data collection cannot be avoided, and this time must be allowed for in subsequent analysis. The amount of time to allow will vary between deployments, determined both by the extent of the temperature differential, and the thermal inertia (Pawlowicz, 2013) of the specific instruments.

The length of time required for thermal equilibration can be reduced by storing instruments as close as possible to ocean temperature prior to deployment. However, for deployments into supercooled water, the additional complexities associated with thermal equilibration can be eliminated if the instrument is stored above the freezing temperature, as this will reduce ice formation in and around the instrument during initial descent.

We recommend allowing instruments to 'soak' at a depth that avoids supercooling and frazil for a length of time sufficient to allow equilibration to proceed. Practically, this is likely to mean soaking as deep as possible so as to reduce the likelihood of ice contamination as far as the pressure-dependence of the freezing point allows. In the case of cooling the SBE19plus down to ocean temperature, a soak of 10 min at 400 m (at which depth the resident water mass in McMurdo Sound is typically High Salinity Shelf Water, which has a temperature of ~ − 1.9 °C) has proven to be sufficient. This significantly exceeds the period for thermal relaxation of 45 s identified by Lueck and Picklo (1990). However, it is identical to the soak time of 10 min of thermal equilibration identified by Lewis and Perkin (1983) working in the supercooled water north of Svalbard.

A similar 'deep soak' procedure can also be beneficial for instruments that are initially cold relative to ocean temperature. However, the length of time required will be significantly greater, as it will be necessary to melt any ice formed on and inside the instrument during its descent through the supercooled layer. High Salinity Shelf Water – the warmest water available in western McMurdo Sound – retains the surface freezing temperature acquired during its formation. Hence its ability to melt ice is limited, being drawn solely from the influence of pressure on the freezing temperature.

3.2. Contamination by ice within the conductivity cell

When profiling or moored instruments that have a conductivity cell (or other sensors that require a known-volume) are exposed to supercooled water, there is a risk of data contamination by ice retention and/

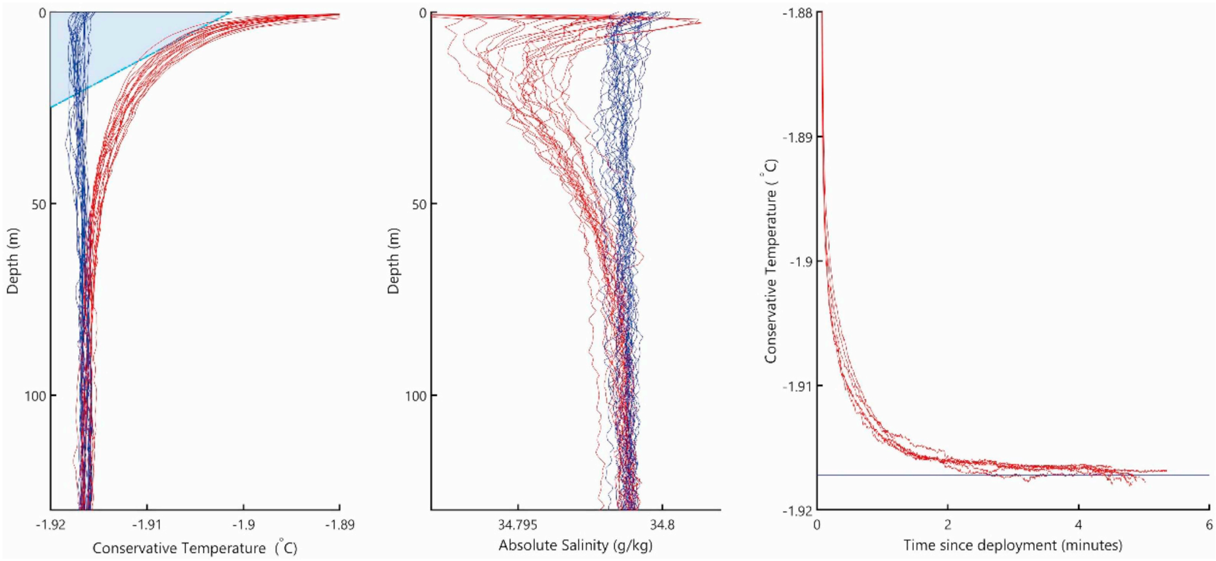

Fig. 4. Sequential half-hourly downcast (red) and upcast (blue) conservative temperature (left) and absolute salinity (centre) profiles. The blue shading identifies the salinity-dependent in-situ freezing temperature. Right: Change in measured temperature with time for each profile until the instrument exited the homogeneous upper layer, with the blue horizontal line showing the mean temperature of this layer from upcast data as a reference point. These data (Set 'A'), collected in 2004 with an SBE-19plus, demonstrate the changes in measured temperature and salinity as the instrument comes to thermal equilibrium over the residual temperature difference of < 2.5 °C after soaking in water at ~ +0.5 °C. It is apparent that the process of thermal equilibration continues beyond 5 min into the deployment. (For interpretation of the references to colour in this figure legend, the reader is referred to the web version of this article.)

or growth within the sample cell. This contamination may occur in two principal ways:

(i) Small frazil crystals may be drawn into the conductivity cell and, to the extent that they displace liquid water, will lead to artificially low conductivity being registered (McPhee et al., 2013). Frazil crystals may be held in suspension over a significant depth range (Leonard et al., 2006), and hence have the potential to corrupt large portions of profile data.
(ii) Ice may adhere and grow on the inner surface of the conductivity cell, particularly in the case of a relatively cold instrument entering supercooled water. This will also reduce the effective volume of the cell, and hence lead to erroneous conductivity measurements (McPhee et al., 2013).

Either of these effects bring an additional risk of complexity through active phase change. This could be realised as either melting or freezing induced by pressure increase or decrease, respectively, which is particularly relevant for a profiling instrument. In addition to changing the effective volume of the measurement sample, phase changes will be accompanied by further changes to both temperature (e.g. release of latent heat with freezing) and salinity (i.e. release of fresh water with melting) within the sample volume.

The nature and significance of the physical contamination will determine the significance of its impact on the data. We interpret large (i.e. > 1 psu) fresh spikes in salinity that occur over one or two measurements as resulting from an individual crystal that is rapidly flushed through the system (e.g. Lewis and Perkin, 1983). In that case it is appropriate to simply remove the affected data points. Longer-lived contamination (see Fig. 5 for examples) results from higher concentrations of crystals in the ambient water, and from processes of melt or freeze within the cell. In such cases it is unlikely that useable data can be recovered.

3.2.1. Identifying and managing data corruption by physical contamination

Contamination by crystal entrainment is a frequent occurrence that, with standard oceanographic equipment, is both unpredictable and uncontrollable. The exception to this is, for profile data, frazil contamination is observed almost-exclusively during descent rather than ascent. As an example of this difference, during a recent (2018) field campaign which featured 299 profiles collected over two 24-h periods, 50 (17%) downcasts were characterised as being contaminated to some extent by frazil crystals, while only 7 (2%) of upcasts were similarly characterised. This difference is most likely due to the physical arrangement of the instrument, particularly the location of the water sampling intake.

Hence, planned data redundancy is critical for providing a basis for comparing data series' and identifying contaminated sections. For profile data where frazil crystals are abundant we recommend collecting multiple sequential profiles (e.g. Skogseth et al., 2009) from which it is possible to identify crystal-induced spikes and hence the uncontaminated water column structure by intercomparison (examples provided in Fig. 5).

For moored deployments, this could be achieved with additional sensors within the anticipated supercooled layer (e.g. McPhee et al., 2013), or with companion profiled data. Alternatively, a system originally devised for active mitigation of physical contamination by ice within the conductivity cell (Morison & McPhee, pers. comm), is being further developed and tested by the authors of the present study. A prototype of the updated system has undergone initial field trials, and its operation and response to supercooled water will be presented in future.

3.3. Anchor ice on suspended equipment

Any equipment introduced to a supercooled environment has the potential to function as a site of concentrated relief of supercooling by ice growth (e.g. Fig. 6). Significant ice growth can cause instruments and sections of moorings to become buoyant (e.g. Mahoney et al., 2011; Craven et al., 2014; Robinson et al., 2014) and cause cyclic and/or cumulative episodes of mooring lift. These can be subsequently identified in pressure records (Fig. 7), as was also observed by Hunt et al. (2003) in Eastern McMurdo Sound.

Naturally-occurring supercooling of ISW observed to date is not sufficient to promote spontaneous nucleation of ice crystals (Daly, 1984). Therefore, relief of supercooling is only possible via enlargement

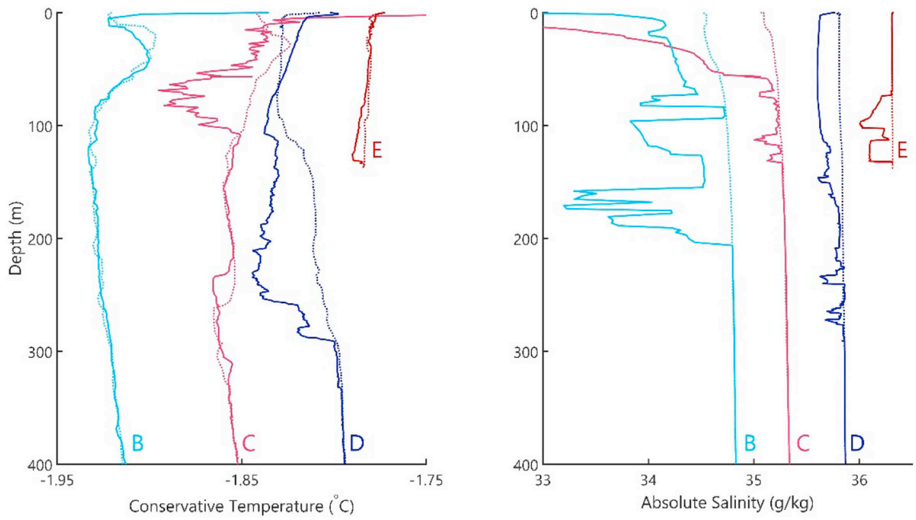

Fig. 5. Examples of corrupted conservative temperature (left) and absolute salinity (right) profiles resulting from contamination within the conductivity cell. Dotted lines represent data assessed (using the methods herein) to be of high quality, while the solid lines represent departures from that. The letters associate each data set with its reference in Table 1, where further details of each deployment are available. Likely causes of the contamination are capture of frazil crystals (data sets B and C), pressure-induced melt of ice within the conductivity cell (data set D), and sediment drawn into the instrument during contact with the seafloor (data set E). For clarity of viewing, potential temperature profiles are offset by 0.06 °C and salinity profiles are offset by 0.5 g kg^{-1}. We note that in certain circumstances, the contamination may only become apparent through comparison with similar and synchronous data (e.g. upcast vs downcast data).

Fig. 6. Growth of ice on rope of top-mounted mooring suspended in supercooled water for 17 days. In this case, the open weave of the polyester rope promoted crystal trapping and growth that mimicked the texture of the rope.

of existing ice – which may be either a contiguous ice cover or crystals suspended in the flow.

However, if the equipment is deployed in the open, and has equilibrated to the ambient air temperature prior to deployment (which may be 5–20 °C below the water temperature), it may be sufficiently cold to trigger crystal nucleation directly onto itself - either through provision of a site for crystal adhesion and growth (Reimnitz et al., 1987; Daly, 2008), or by sufficiently cooling water (i.e. to > 1 K supercooled) in the immediate vicinity to allow spontaneous nucleation to occur. Additionally, even when equipment introduced to the environment has been relatively warm (i.e. above freezing temperature) prior to deployment, the observed accumulation of ice demonstrates that ropes, frames and instruments also provide sites for suspended ice crystals to settle and concentrate (i.e. a crystal 'trap'). Our experience with both types of deployment indicates very little difference in ice accumulation between 'warm' and 'cold' deployments, suggesting that the role of suspended equipment as a crystal trap is more effective than its potential role as an introduced site of ice nucleation.

3.3.1. *Influence of equipment texture surface*

Unsurprisingly then, the effectiveness of the crystal trap depends on physical properties of the equipment. Two separate mooring deployments within the supercooled outflow (data sets F.

and G), which were subject to similar ranges of temperature, salinity and tidal flows (Table 1), highlight the potential influence of the rope's texture:

In the most severe example of ice growth on an oceanic mooring line reported to date (data set F, Table 1 and Fig. 3; collected in 2007 and initially reported by Robinson et al., 2014), a top-mounted mooring with a net weight of 90 kg was lifted a total of 80 m over just 15 days. In that case, the rope used was open-weave 12 mm polyester, and the pattern of ice growth imitated the texture of the rope itself (Fig. 6). With a continual flow of supercooled water past the site, the crystals grew rapidly larger while remaining firmly secured in place within the structure of the rope. After an initial period of 2½ days, the accumulated buoyancy was sufficient to overcome the weight of the mooring, causing the instruments to rise through the water column.

Only 3 ½ and 8 ½ days into the deployment, the upper and middle instruments (initially deployed at 15 m at 50 m respectively) became incorporated into the sub-ice platelet layer, and no longer sampled the target depth (Fig. 7, pink shades). In their original presentation of these data, Robinson et al. (2014) inferred that the mean radial rate of solid ice growth over the upper 70 m of line must have been ~2 cm per day in order to achieve neutral, and subsequently positive, buoyancy.

In contrast, no cumulative uplift trend was evident for the 2016 mooring (data set G; Fig. 7 blue shades), despite the equipment being located much closer to the ice shelf front and exposed to a deeper supercooled layer (i.e. ~90 m vs ~70 m). In that case, a dyneema line was used to deploy a similar instrument load (Fig. 3) for a period of 14 days. Mooring lift by ice growth was apparent in multiple episodes, between which the instruments returned to their initial deployment depths very rapidly (i.e. within 2 min; Fig. 7, blue shades). This suggests that the

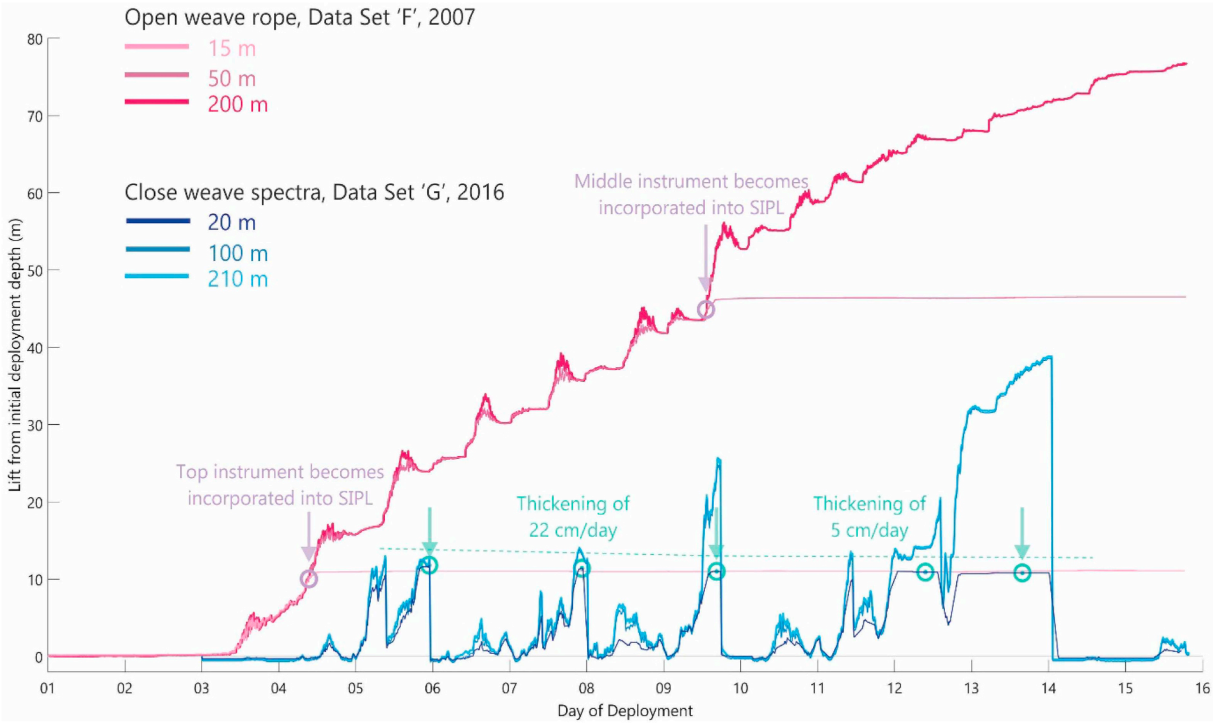

Fig. 7. Different patterns of buoyant lift from employing open-weave polyester rope (pink traces, data set F) and 6 mm dyneema cable (blue traces, data set G) to suspend instruments, as demonstrated by pressure records from three SBE-37 microcats for each deployment. For clarity, buoyant lift is shown as the change in instrument depth (i.e. initial deployment depth, indicated in the legend, subtracted from recorded depth) as a function of time in days. It is apparent that, after an initial period of ice growth, data set F was subject to cumulative lift, superimposed over which was apparent tidal variability. The lift was sufficient that the upper two microcats, initially deployed at 15 m and 50 m, both became lodged within the sub-ice platelet layer (SIPL) at the top of the water column – after which no change to pressure was recorded. In contrast, data set G was subject to episodic lift that was not cumulative, indicating that ice accreted onto the cable was periodically dislodged, thereby allowing the instruments to rapidly return to their initial deployment depths. In five of these episodes, the minimum depth attained by the top-most instrument was static for a short period which is taken to represent the position of the platelet layer base. Sequential change in depth attained thereby represents thickening of the platelet layer by accretion of additional crystals. This equated to thickening of 22 cm day^{-1} over the first period of the record and 5 cm day^{-1} over the second period, which reflects the degree of supercooling observed by the microcat deployed at 100 m. (For interpretation of the references to colour in this figure legend, the reader is referred to the web version of this article.)

accumulated ice was only very loosely attached to the exterior of the rope.

This interpretation is supported by observations made on other occasions when similar cable has been used. On those occasions, the observed pattern of ice growth bore no similarity to the rope's weave, but more closely resembled the random arrangement of platelet crystals within the sub-ice platelet layer (see Fig. 7 of Robinson et al., 2014). This leads to the conclusion that the attachment of frazil crystals is random, and subsequent growth far more tenuous, for close-weave cable compared to open-weave polyester.

Finally, significant ice accumulation has also been observed on both instruments and their steel frames following deployment in supercooled water. It is apparent that a smooth and contiguous surface (e.g. Nortek Signature current profiler, Deployment 'H', Fig. 3) does not promote ice adherence or accumulation. In contrast, the discontinuous surfaces of microcats and CTD profilers present multiple sites for trapping ice crystals, promoting attachment and subsequent bonded growth (Fig. 8). In addition, attachment of ice crystals to frames engineered for such deployments is clearly initiated and concentrated at welding points, although this could be avoided if care is taken to ensure a smooth finish. This accords with the general conclusion that anchor ice will accumulate only when the substrate is coarse (Reimnitz et al., 1987).

3.3.2. *Preventing or reducing ice accumulation on sampling equipment*

Accumulation of anchor ice can limit the effectiveness of an oceanographic mooring in four direct ways:

(i) it shifts the location of observation from the intended depth to a lesser depth in a way that cannot be predicted or controlled, via buoyant uplift and increased current drag imposed against an increased upper ocean expression of the mooring through ice accumulation.
(ii) it increases the likelihood that the data will become corrupted by crystals trapped in or near the sensors;
(iii) the instrument may become incorporated into the continual downward extension of the sub-ice platelet layer by crystal accumulation; and
(iv) in severe cases, ice build-up may be sufficient to prevent recovery of the equipment.

Hence any solution that minimises ice accumulation will extend the useful life of a mooring deployment. The following preventative measures are recommended, although not all may be appropriate for all situations:

- The surface roughness of suspended equipment determines its ability to support ice growth. Hence, in the first instance, we recommend using smooth, close-weave ropes or smooth plastic jacketed wire, which follows from the experience of our moorings deployed in 2006 and 2017 (described above, and with further detail provided by Robinson et al., 2014). In addition, attention should be paid to, as far as possible, ensuring the smoothness of joins in welded frames and instrument surfaces. Both of these measures reduce the potential of the suspended equipment to act as a crystal 'trap' by providing surfaces onto which suspended frazil would be able to settle and adhere (Reimnitz et al., 1987; Daly, 2008).

Fig. 8. Ice attachment and accumulation after 3 days of top-mounted deployment in supercooled water. On recovery, it was apparent that the initial ice attachment and subsequent growth was concentrated on the relatively rough transducers of a Nobska MAV and on connection points of the steel frame. In contrast, minimal ice attachment occurred on the smooth and contiguous surfaces of the Nortek Signature current profilers, although in this case, contiguous growth encroached into the immediate vicinity of the upward-looking Signature.

- For mid-length deployments, buoyant rise due to ice accumulation (e.g. Hunt et al., 2003; Craven et al., 2014; Robinson et al., 2014) may be crudely countered by the addition of more ballast weight during deployment. This action will not prevent any ice build-up but will delay the point at which uplift begins. The effectiveness of this measure will depend on the depth and degree of supercooling exposure, and the propensity for suspended equipment to accumulate ice. As detailed above, 70 kg of ballast was sufficient to prevent lifting for only 2 ½ days in 2006. In contrast, similar ballast allowed 18 days of continuous data collection in 2017. We note that additional ballast can make manual handling of the equipment more challenging, particularly during recovery, and the overall response may be complex due to the change in drag profile of the suspended equipment.
- For longer top-mounted deployments the only practical solution may be to periodically remove accumulated ice. This may be achieved manually, via a repeated cycle of recovery, de-icing, and redeployment. The frequency of de-icing required will depend on the supercooling conditions. In recent deployments in Western McMurdo Sound swamping by ice accretion rendered the instruments ineffective after only 30 h (as shown in Fig. 8). However, as noted above, this inundation could be planned as a 'sacrificial' deployment where regular de-icing is not feasible (ref to Fig. 9 and the point at which instruments become encased). Alternatively, if revisiting the equipment on multiple occasions is not practical, some form of autonomous removal may be possible. Testing of new devices designed for this purpose is planned for future field work.
- We anticipate that bottom-mounted mooring or autonomous profiling arrangements are the surest way to eliminate data contamination by ice growth in supercooled water. These could be deployed from research vessels, but the authors are unaware of any moorings either deployed in this manner in McMurdo Sound or in supercooled water elsewhere in Antarctica. The landfast ice in McMurdo Sound makes this a logistically challenging but scientifically attractive proposition, and we are presently developing this capability.
- A fifth, as yet untested, potential solution, is to modify instrument surfaces to become icephobic using nanotechnology. Such targeted modification has been successfully applied in applications as diverse as aviation (Kim et al., 2012), wind turbines (Zhang et al., 2017) and power lines (Golovin et al., 2016), but to the authors' knowledge has not yet been trialled for oceanographic conditions.

3.4. Ice coating of sensors

Instruments suspended in water whose temperature is sustained below the in-situ freezing point risk becoming ineffective due to the restriction of flow to the sensors and resultant localised ice accumulation and growth. Attachment of anchor ice near sensors has two potential modes of corruption, neither of which are necessarily obvious on inspection of the data.

(i) Sensors may gradually or rapidly become completely encased in ice, and thereby become insulated from natural high-frequency variations in the ambient flow; and
(ii) Latent heat released due to artificial and highly localised ice growth can raise the sensed temperature towards the in-situ freezing point.

In a 2017 deployment (data set I), five temperature sensors (a combination of SBE-56 thermistors and SBE-37 microcats with 70 kg of ballast; Fig. 3,) were spread throughout the supercooled portion of the homogeneous upper ocean boundary layer beneath the sea ice of Western McMurdo Sound. The degree of supercooling each instrument was exposed to decreased with increasing depth, owing to the pressure-dependence of the freezing temperature in a homogeneous water column. Hence their encasement in ice, signalling the end of their useful deployment, occurred sequentially (Fig. 9). The point of full encasement could be identified by a substantial reduction in the temporal variability of both temperature and salinity (Fig. 9), a feature that was also reported by Robinson et al. (2014); data set F in the present study).

Immediately preceding the inferred point of encasement, each instrument registered warming of ~0.01 °C – a change that was not reflected in the records from the remaining instruments. This is significant as, while the sensors were fully exposed to the ambient flow, they simultaneously registered property changes, reflecting the homogeneous nature of the upper ocean in this location. Thus, an individual instrument behaving differently was responding to a process uniquely observed by the sensor in question, and which immediately preceded full encasement. We therefore interpret this warming as registering the latent heat released in the immediate vicinity of the sensor as it became encased in ice. The measured heat released may provide an indication of the local strength of turbulence diffusing heat and salt away from the growing interface and controlling the local ice growth rate.

During periods in which the sensors were encased in ice, not only did the variability in measured properties reduce dramatically, but the subsequent recorded temperature reflected the pressure-dependent freezing point local to the deployment depth. This can be clearly seen in the sustained difference in temperature of the upper three instruments (blue traces in Fig. 9). The difference in conservative temperature of ~0.01 °C between adjacent instruments corresponds to the difference in in-situ freezing temperature at their local deployment depths. This interpretation is, serendipitously, straightforward because the mooring was not substantially affected by buoyant lift by ice accumulation (red traces, Fig. 9). This process occurred repeatedly throughout the deployment, with each instrument returning to its pressure dependent freezing point after ice growth (note horizontal arrows representing periods of ice encasement in Fig. 9).

Our data demonstrate, by the remarkable homogeneity of oceanographic properties with depth of uncorrupted data, that it is possible to recover reliable records from water that is supercooled to the observed degree (i.e. < 50 mK; for example, compare green (40 m) and grey (75 m) traces of Fig. 9). The length of useful record obtained depends on the degree of in-situ supercooling the instruments are exposed to, which in turn, is strongly influenced by the depth of deployment. As a clear example of this, a difference in depth of just 10 m generated a difference in useful record length of 1 day (light blue trace, Fig. 9) compared to 6 days (green trace).

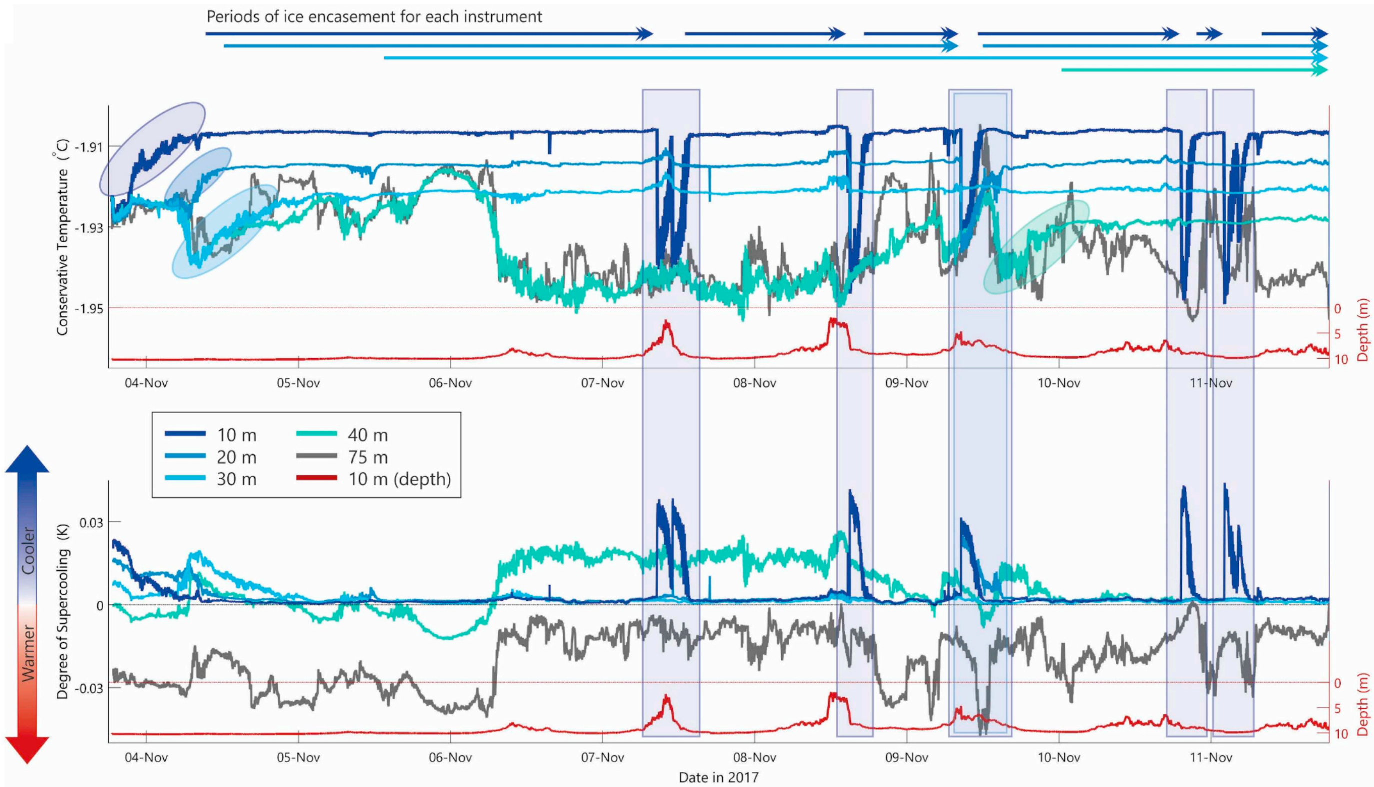

Fig. 9. Conservative temperature (top) and degree of supercooling (bottom) as measured by five instruments (data set I) simultaneously suspended in supercooled water (depths of each indicated by colour key) as well as depth (red) of the top instrument (right hand axes). Sequential and repeated episodes of ice encasement of the top four sensors (colour-coded ellipses) were identified by apparent warming (registering the very local release of latent heat) which was followed by very low variability in signal (reflecting the effective insulation from ambient water by ice on the sensor). These events were accompanied by small changes in pressure due to the buoyancy of the growth on instruments and lines. Episodically, the ice encasing the top instrument came away, which briefly exposed the sensor to the ambient temperature. Warming, also indicated by a reduction in supercooling (vertical arrows), occurred immediately as ice rapidly reformed around the sensor following each episode. The colour-coded horizontal arrows at the top of the figure show the periods for which we conclude that each sensor was encased in. (For interpretation of the references to colour in this figure legend, the reader is referred to the web version of this article.)

3.4.1. Managing ice encasement and release of latent heat

To avoid the data contamination caused by ice encasement and the release of latent heat we recommend that instruments should be deployed at as great a depth as possible – which will access a lesser degree of supercooling – and where feasible to replicate the measurement at multiple depths (as applied by McPhee et al., 2013).

We recommend that data from moored deployments in supercooled water should be carefully inspected for corruption by ice encasement and induced release of latent heat. In an earlier application of this protocol Skogseth et al. (2009) completed this inspection in consultation with the calibration experts at Sea-Bird Scientific. Such attention to detail demonstrates that the signatures of these effects are not necessarily obvious. However, for most situations, we suggest that these subtle forms of corruption can be identified by comparison of records collected simultaneously at different depths, or via complimentary full-depth profiles.

4. Discussion

The issues and their recommended management strategies identified above should be considered in all deployments for which contact with supercooled and/or frazil-laden water is possible. In the next sections, we expand the discussion of ice nucleation in the sub-ice environment, provide an example of how one mode of 'corruption' was exploited to gain more information about the system, and discuss how sensor type and timescale might generally influence these issues. We then present a complete procedure for CTD profiling in supercooled water, before discussing how the range of recommendations may be expanded for application to other platforms.

4.1. Sources of ice nucleation and subsequent frazil explosions

From the comprehensive review by Daly (1984), it is evident that neither form of primary nucleation can occur with natural levels of supercooling in the marine environment, and hence some form of seeding is required. Where mass exchange with the atmosphere is possible, snowflakes or ice particles introduced from elsewhere may provide the seed stock (Daly, 1984). In addition, splashes, windspray or bursting of bubbles at the surface may allow tiny droplets of slightly supercooled fluid to be rapidly cooled further by the atmosphere, and return to the ocean as ice crystals, typically requiring air temperatures of −9 to −8 °C (Osterkamp, 1977).

However, in the absence of mass exchange with the atmosphere, as is the case beneath a contiguous ice cover (either sea ice or ice shelf), it is not clear what the original source of seeding is. Some studies report spontaneous nucleation of frazil in supercooled water (e.g. Foldvik and Kvinge, 1974, 1977). However, with reference to the conditions required for primary nucleation (Daly, 1984), these observations must be discounted as having included ice seeds that were too small to be visible to the naked eye or filtered out, but which are nonetheless detectable by strong light under laboratory conditions (e.g. Michel, 1963).

In searching for the ultimate source of nucleation beneath ice covers, some authors suggest that crystalline growth directly onto the sea ice or ice shelf base may provide suspended nuclei following shearing off by boundary flows (e.g. Clontz and McCabe, 1971; Daly, 1984). Alternatively, mechanisms involving sediment-laden and relatively fresh sub-glacial discharge under pressure (e.g. Tweed et al., 2005; Morozov et al., 2015) may be responsible, but these remain unobserved in the Antarctic. Makkonen and Tikanmäki (2018) propose seeding mechanisms that are fully contained within the fluid, such as cavitation and microbubbles. However, their experiments required supercooling near 1 K to support these modes of nucleation – which, for practical applications in natural water bodies, would make these mechanisms indistinguishable from heterogenous nucleation as described by Daly (1984).

Beginning from the model of frazil ice dynamics presented by Daly (1984), the dynamic balance of ice crystal growth in supercooled water has been explored via numerical simulation in increasing levels of complexity by Omstedt and Svensson (1984), Omstedt (1985), Holland and Feltham (2005), Wang and Doering (2005), Daly (2008) and Rees Jones and Wells (2018). At the simplest level growth of ice crystals in supercooled water releases latent heat which draws the bulk temperature towards the in situ freezing point, effectively quenching supercooling. However, there are a number of interacting and interdependent processes that complicate this behaviour: Wang and Doering (2005) identified that particle growth, flocculation and break-up, gravitational removal, initial seeding of ice crystals, and secondary nucleation must all be incorporated in order to accurately simulate relief of supercooling to suspended crystal growth.

Going into greater detail, Rees Jones and Wells (2018) explored the processes that lead to the occurrence of 'frazil-ice explosions' which can rapidly reduce the level of supercooling to a small residual amount. This accords with the observations of Carstens (1966) and Muller (1978) under controlled laboratory conditions, although those authors were not able to identify or quantify the process involved.

Rees Jones and Wells (2018) identified three environmental controls that promote frazil explosions through specific mechanisms: (i) greater turbulent intensity, which increases the rate of secondary nucleation, (ii) increasing the mixed layer depth, which reduces the rate of gravitational removal, and (iii) increasing the cooling rate which both increases the growth potential and the likelihood of secondary nucleation through larger crystal sizes. They further identified that the treatment chosen to represent growth of suspended crystals radically affects predictions of basal accretion and behaviour of the supercooled plume, with implications for predicting the evolution of ISW plumes.

4.2. Opportunistic observations

While mooring lift by anchor ice accumulation is both undesirable and unsystematic, during some deployments in supercooled ISW it has allowed opportunistic post-deployment analysis that would not have otherwise been possible. An example is the indirect measurement of sub-ice platelet layer thickening observed in 2016 (data set G, Fig. 7). For that deployment, the upper-most instrument, an SBE-37 microcat, was nominally deployed at 10 m below the base of the sub-ice platelet layer. It was expected that the instrument would become encased in ice, and therefore become ineffective soon after deployment. This 'sacrificial' deployment was necessary to determine the true degree of surface supercooling, even if it meant that the uncorrupted record was only 1 or 2 days long.

On recovery, it was noted in the pressure record (Fig. 7) that on five occasions the instrument had risen to a temporarily-stable depth before ice on the line was evidently rapidly released and the whole mooring returned to its original deployment depth (Fig. 3). We interpret this stable depth as representing the position of the sub-ice platelet layer base and were therefore able to estimate its thickening over the 13-day deployment, albeit infrequently. The inferred rates of platelet layer extension (22 cm/day and 5 cm/day over consecutive 4-day periods; Fig. 7) reflected the changing temperature, and hence degree of supercooling, as measured by uncorrupted instruments suspended deeper in the homogeneous upper ocean layer. They also correspond with estimated mean thickening of 3.5 cm/day over 23 days from repeated remote sensing of the sub-ice platelet layer conducted around the same time (pers. comm. G. Brett).

In another example, it has also been noted that ice crystals suspended in supercooled water can interfere with acoustic fish-finders and cause erroneous returns in remotely-sensed ice thickness measurements. In recent years, these modes of 'interference' have been exploited to actively search for and characterize sub-ice platelet layers (e.g. Rack et al., 2013; Hunkeler et al., 2016) and suspended frazil populations (e.g. Leonard et al., 2006).

4.3. Effect of sensor type

The type of sensor deployed will determine the degree to which thermal equilibration, ice within the sample volume, and coating of sensors by ice could contaminate the data. For T/S measurements, there are two basic choices to be made, according to the type of deployment: (i) whether or not to use a pump to direct and control flow of the sampled water past the sensors and (ii) whether to measure conductivity by electrical resistance or induction. To our knowledge, there are presently no conclusive data available that have been collected specifically for determining the response of these different sensor types in frazil-laden supercooled water, although both of these are ongoing avenues of investigation for the authors.

We anticipate that where conductivity is measured by electrical resistance, a pumped instrument (such as the SBE19plus used here) would minimise corruption by thermal equilibration (by reducing the time required for this process to proceed) and by ice growth (by flushing the crystals through the system faster).

Whether it is better to use electrical resistivity or induction to measure conductivity in supercooled and frazil-laden waters remains unclear. Direct comparisons between the SBE19plus (pumped, resistance measurement) and the RBR-Concerto (unpumped, inductive measurement) in test profiles by the authors (2018) have yielded small but significant, and apparently unsystematic, differences in measured temperature and salinity. The origins of the discrepancies are not yet clear but may be related to the instruments' stability in frazil-laden water and its relation to the high degree of precision required in supercooled waters.

4.4. Timescales of corruption

The significance of each of the issues identified above varies with the type and timescale of observation (Fig. 10). For data collection by profiling allowing time for thermal equilibration will be necessary, as the timescale of equilibration can be significant compared to that of the deployment (e.g. Lewis and Perkin, 1983). On the other hand, new ice growth is unlikely to be significant within the timeframe of exposure to supercooled water during full- depth profiling, so buoyant lift and latent heat contamination are less likely to require resolution.

Moored deployments could potentially be exposed to all four modes of contamination identified here, but it may be straightforward to deal with those that have shorter timescales (e.g. thermal equilibrium and contamination by individual crystals) by eliminating affected data in post-deployment processing (e.g. Drucker et al., 2003). In that case, it is the longer-lived issues that pose the more significant threat to data quality.

In addition, collection of simultaneous data (e.g. supplementing moored data with pre- and/or post-deployment water column profiling, or repeating observations at multiple depths) may allow instances of supercooling to be reported with careful reference to them (e.g. Skogseth et al., 2009; McPhee et al., 2013; Robinson et al., 2014). Where companion data are not available, it may be necessary to significantly revise the apparent degree of supercooling (e.g. Kirillov et al., 2018), although this approach significantly increases the uncertainty in supercooling characterisation.

4.5. Recommended protocol for CTD profiling in supercooled and/or frazil-laden water

Our experience has prompted the development of a working protocol for CTD deployments when supercooled water may be present: We begin

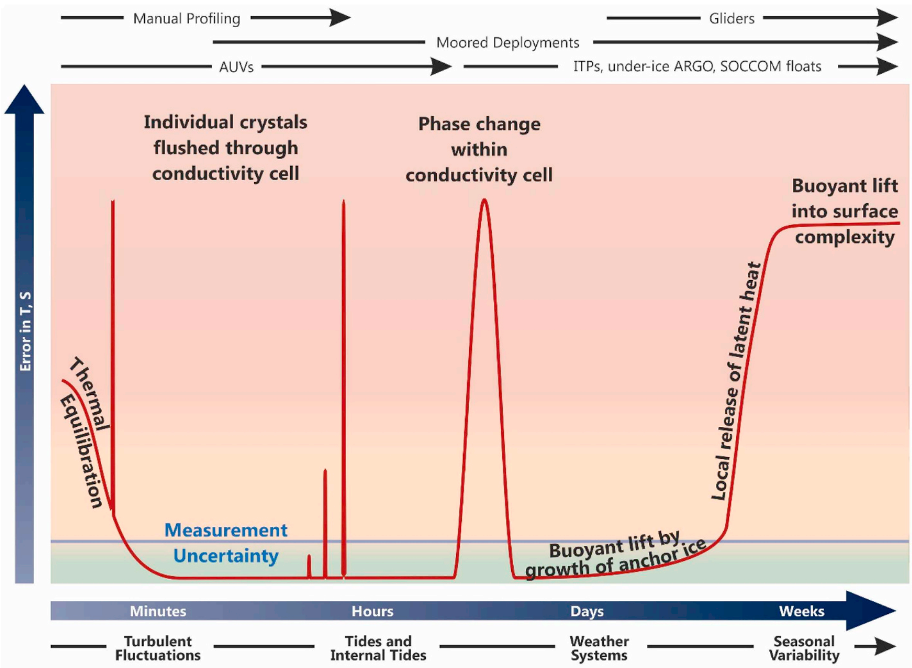

Fig. 10. Timescales for various modes of potential data corruption identified in the text. The horizontal axis indicates the time periods during which each mode of corruption is likely to be most significant, while the vertical axis indicates the severity of the corruption as manifested in errors of measured temperature and salinity. These can be related to the various platforms for data collection, as well as the timescales for various natural sources of.

with a "soak" of 10 min near the seafloor, followed by continuous sampling through two complete upcast-downcast cycles (for example cast, Data Set J, see Fig. 11). This should be completed without bringing the instrument out of the water (e.g. Block et al., 2019) as exposure to the colder atmosphere could allow rapid crystalisation of water on and inside the instrument. This then yields a total of five casts (2× downcasts, 3× upcasts) that are available for subsequent analysis. Direct comparison of the five profiles will reveal whether any have been subject to corruption via frazil retention or phase change, by looking for inconsistencies between profiles.

Caution is advised with the inclusion of upcast data in analysis, as this may represent an additional source of measurement bias, determined by the instrument's configuration. However, any such error is likely to be 2–3 orders of magnitude smaller than that introduced via the modes of corruption identified in this study (Fig. 10; SeaBird Electronics, 2017) Thus, upcast profiles at least provide useful reference data for identifying possible modes of corruption in CTD profiles. A practical way forward may be to use upcast data to demonstrate that downcast data are free from corruption due to instrument response and then to eliminate them from subsequent analysis.

It also possible – and advised by the manufacturer for certain types of deployment – to invert the orientation of the SBE19plus, so that the temperature and conductivity sensors at are the top – in which case downcast data should be ignored (SeaBird Electronics, 2017). This has not yet been trialled by the authors for deployments in supercooled water but will be assessed as a possible alternative solution in future deployments.

4.6. Extension of recommendations for other platforms and applications

Beyond the traditional platforms identified above, autonomous vehicles and marine mammals are providing a step change in access to the polar oceans, and corresponding orders-of-magnitude increase in rate of data collection. Such platforms typically combine aspects of profiling and moored experiments and may be exposed to multiple modes of corruption equally and repeatedly. Complexities arising from contact with supercooled water therefore pose considerable risk to instrument recovery and data quality (Fig. 10). In all phases of planning, deployment and data analysis, careful consideration of the issues identified

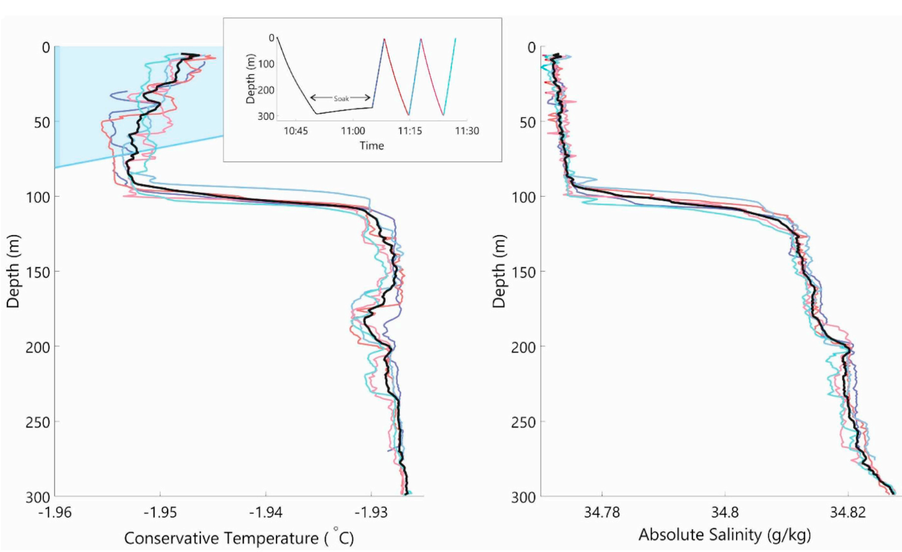

Fig. 11. Full-depth profiles of potential temperature (left) and salinity (right) collected in 2017 using the sampling protocol recommended here (data set J). Individual casts are colour-coded as indicated by the pressure timeseries (inset), and mean profiles are shown in black. Inset: the pressure timeseries for the recommended profiling protocol, including initial soak at depth to allow thermal equilibration to proceed without phase change and multiple vertical traverses of the water column to assist with identifying and removing corrupted data points.

here is critical for a successful observational programme. Recommendations specific to these platforms are provided below.

4.6.1. Through-ice shelf deployments

The sub-ice shelf cavities of Antarctica comprise a range of oceanic regimes that include grounding line and pinning points, marine ice accretions, inverted crevasses, ice stream convergence and frontal regions. They incorporate vast areas that have never been directly observed, and hence much of the interface complexity and upper ocean structure remains to be quantified. We therefore expect that the following recommendations will evolve as familiarity with these areas increases.

Ice Shelf Water, the source of supercooling in the present study, is a modification of High Salinity Shelf Water following interaction with an ice shelf at depth. Hence, naturally-occurring pressure-induced supercooling is expected only in the coldest cavities or those with a thick ice cover. In these situations, thermodynamic processes that disrupt the delicate supercooling balance could be activated by the process of gaining access to ice shelf cavities.

Some grounding line areas are known to be influenced by terrestrial run-off from rivers or sub-glacial melt. These may deliver water that is very cold (if the terrestrial storage has sufficient pressure applied via overlying ice) relative to the ocean and/or laden with sediment. On contact with ocean water already at its in-situ freezing temperature, such a confluence could allow the affected ocean water to become supercooled (e.g. Tweed et al., 2005; Morozov et al., 2017), or drive explosions of crystal nucleation (Muller, 1978; Rees Jones and Wells, 2018). In such a delicately-balanced system, it may prove difficult to distinguish naturally-arising two-phase complexity from that artificially initiated by creating access and introducing instruments to the environment.

Hot Water Drilling is presently the most common method used to gain access to sub-ice shelf cavities. However, the water used and produced in melting access may itself create issues, having a propensity for rapid freezing, as it is trapped within the borehole, in close association with the ice itself. For this reason, the soak required to achieve thermal equilibrium should not be completed within the access hole but as far beneath the ice-ocean interface as possible. The heavy equipment required for Hot Water Drilling may provide further opportunity to avoid contamination by ice growth by modifying or exchanging the tether used to suspend the instrument, since manual handling could be eliminated. This may include using Teflon-coated wire applying an ice-phobic grease/lubricant coating or even applying minimal heating to the wire via a surface unit, but these methods remain to be trialled.

4.6.2. Bottom-mounted moorings

If deployed in sufficiently shallower waters, the seafloor unit of a bottom-mounted mooring may be at risk of inundation by anchor ice. If this occurs, it will only be a matter of time before the anchor becomes buoyant and the mooring is lost. Even on shorter timescales, caution with shallow bottom-tethered instruments is advised as ice build-up may interfere with release mechanisms or tethering arrangements.

For deployments in deeper water, where the risk of anchor ice formation is non-existent, the upper sections of the mooring string could still be subject to ice formation on instruments, frames and/or ropes. This puts the collection of quality data at risk, as outlined above. For long-term moorings we therefore recommend suspending instruments (or equipment) strictly below the supercooling horizon.

4.6.3. Surface-based operations on the open ocean or beneath ice

For vessel-based operations in polar waters, it may not be necessary for the ocean water to be near or below its freezing temperature for data to be corrupted as described above. Instruments stored on deck, and hence exposed to atmospheric temperatures that may be many degrees below freezing, will be cold relative to the ocean on deployment. The temperature differential is large in such a scenario and therefore may induce ice formation on and/or inside instruments and equipment during deployment. Storing instruments in heated boxes (e.g. Skogseth et al., 2009), or deploying them from heated environments (e.g. Albrecht et al., 2006) will help in reducing this form of corruption.

Exposure to cold air is also a potential issue on recovery: any liquid water remaining on or inside the equipment will rapidly crystallise on recovery. This introduces solid material to critical areas, such as seals, which may therefore become ineffective on redeployment, resulting in flooded equipment. On longer exposure to cold air, the expansion associated with ice formation could also cause conductivity cells (or similar) to rupture. We therefore recommend that equipment used in multiple deployments (e.g. repeat CTD casts) under conditions of very cold air temperatures is kept below the water's surface between casts (also recommended by Block et al., 2019). If this is not possible, the instrument must be allowed to warm and/or drain as appropriate between consecutive deployments, as is common practice for many cold-water applications (e.g. Skogseth et al., 2009), thereby eliminating the risk associated with expansion during crystallisation.

4.6.4. Autonomous platforms

The introduction of autonomous observational platforms, such as under-ice Argo, Ice-Tethered Profilers (ITPs), Autonomous Underwater Vehicles (AUVs), gliders, and floats such as SOCCOM (Southern Ocean Carbon and Climate Observations and Modeling project) floats and SWIFT (Surface Wave Instrument Float with Tracking) buoys to the polar oceans has increased data collection there by orders of magnitude. This exciting explosion of information has come at a cost to resolution in depth, location, and measured parameters, immediacy of response, and control over the regimes encountered. Where these navigate near ice shelves, and particularly towards the surface where the risk of encountering supercooling is greatest, an autonomous instrument may be at risk of multiple exposures to all forms of corruption over the course of a single deployment.

Should an autonomous platform stray into a region of in-situ supercooling, it is put at risk of all the potential sources of corruption identified above, but without the immediate knowledge of, and capacity for mitigation by, the researcher. In addition, growth of ice may interfere with location systems (which also adds uncertainly to the likelihood of encountering supercooled water) and buoyancy algorithms, potentially putting the ultimate recovery of equipment and data at risk.

We therefore recommend that a dynamic algorithm should be employed to restrict or eliminate time spent in supercooled water. Although this means a reduction in opportunity for data collection, it is likely to have the added benefit of avoiding contact with physical complexity such as suspended frazil or platelet ice. Where autonomous equipment will be 'parked' at some depth for long periods during its deployment, this should be programmed to be sufficiently deep to avoid supercooled water.

Post-deployment checks on the both the instrument and data recovered should include signs of contamination through contact with frazil-laden and/or supercooled water as outline above. This requires redundancy of data, which should be planned for in the pre-deployment phase.

4.6.5. Animal-borne instrumentation

The application of miniature sensors to animals offers even greater temporal and spatial opportunities for data collection. However, this is accompanied by complete relinquishing of control over where and when data are collected. In processing such data, we recommend thorough and careful analysis wherever near-freezing conditions are suspected for the sources of instrument corruption identified above. The researcher should be aware that this may prove impossible to satisfactorily achieve if comparative data are not available.

5. Concluding remarks

Direct encounters of near-freezing or supercooled ocean water are set to increase due to (i) enhanced capability for gaining direct manual access to ice-covered oceans, (ii) the advent and expanding use of autonomous observational platforms, including floats and mammal-borne instrumentation, and, in the long term, (iii) warming oceans further eroding cold cavity ice shelves and thereby expanding the supply of ISW. Hence, the need to develop suitable protocols for observing supercooled water is becoming increasingly urgent. Agreed protocols need to be developed with the joint aims of (i) reducing or eliminating data corruption via instrument response through optimal instrument handling, and (ii) identifying and eliminating corrupted data before it is used in data analysis or regime characterisation.

Through pressure relief, ISW can become supercooled, which is a metastable state. That is, its maintenance in a natural environment relies on sustaining a delicate balance of temperature, salinity, pressure and suspended crystal concentration. Correct characterisation of in-situ supercooling is therefore possible only if the measurement itself does not disturb this balance by introducing, or erroneously inferring, changes of phase.

Here we have discussed four issues frequently encountered when deploying instruments into near-freezing or supercooled water. In the order that these are likely to be encountered they are: (i) an extended process of thermal equilibration, (ii) contamination by ice within the conductivity cell, (iii) anchor ice accumulation on suspended equipment, and (iv) ice coating and resulting sensing of artificially-produced latent heat.

The issue of thermal equilibration can be simply countered by a soak in a non-supercooled portion of the water column for 10 min (assuming the instrument is initially warm) prior to intentional data collection. The issues involving ice contamination of the sensors themselves (i.e. ii, and iv) may only be identifiable by comparison with simultaneously-collected data, and we therefore stress the need for planned data redundancy in this sensitive environment. In some cases, this comparison may demonstrate that data cannot be satisfactorily rescued and must therefore be omitted from subsequent analysis.

The issue of buoyant lift of moored equipment due to accumulation of anchor ice (iv) is related to the roughness of the substrate, which determines the likelihood of crystal settling and adhesion. We therefore recommend attention to ensuring smooth surfaces and using a tightly woven line for suspension. Where these modifications are not possible, periodic de-icing of equipment or application of additional ballast can extend the useful life of deployments.

We have also made recommendations on how our experience gleaned from top-mounted deployments from land-fast sea ice can be extended to other applications in near-freezing waters. Common to all platforms is the need for planned data redundancy in order to improve the likelihood of collecting uncorrupted data, and exhibit consistency between related data series', which is necessary for demonstrating that the data are indeed free from contamination and suitable for characterising supercooling in a delicately-balanced environment.

Declaration of competing interest

The authors declare that they have no known competing financial interests or personal relationships that could have appeared to influence the work reported in this paper.

Acknowledgements

This work has been funded through New Zealand's Marsden Fund, Deep South National Science Challenge, and the National Institute for Water and Atmospheric Research (NIWA). Logistical support has been provided by Antarctica New Zealand. The authors would like to thank two anonymous reviewers for insightful and highly constructive comments on earlier versions of this manuscript. We also thank Drs Kim Martini (Sea-Bird Scientific) and Clark Richard (Fisheries and Oceans Canada) for guidance on the application of TEOS-10 in this sensitive environment. We thank our colleagues Dr. Tim Haskell, Prof. Pat Langhorne, Matt Walkington and Dr. Greg Leonard for assistance in the field, in developing instrumentation, and for useful discussions over many years.

Appendix A. Precision and accuracy of instruments used in this study, according to their manufacturers

Instrument ID	Purpose	Manufacturer	Resolution	Accuracy	Further information
SBE19plus	Profile	SeaBird	0.00005 S/m 0.0001 °C 0.002% of full scale pressure range	± 0.0005 S/m ± 0.005 °C ± 0.1% of full pressure scale range	https://www.seabird.com/profiling/sbe-19plus-v2-seacat-profiler-ctd/family-downloads?productCategoryId=54627473770
SBE37-SM	CTD, moored	SeaBird	0.00001 S/m 0.0001 °C 0.002% of full scale pressure range	± 0.0003 S/m ± 0.002 °C ± 0.1% of full pressure scale range	https://www.seabird.com/moored/sbe-37-sm-smp-smp-odo-microcat/family-downloads?productCategoryId=54627473786
SBE56	T, moored	SeaBird	0.0001 °C	± 0.002 °C	https://www.seabird.com/sbe-56-temperature-sensor/product-downloads?id=54627897760
RCM	Single-point current meter, moored	SeaGuard	0.1 mm/s 0.01°	± 0.15 cm/s ± 5° for 0–15° tilt	https://www.aanderaa.com/media/pdfs/Seaguard_RCM-TD262b_001.pdf
Sn1000	3-D velocity profiler (1000 MHz)	Nortek	0.1 cm/s	± 0.5 cm/s	https://www.nortekgroup.com/manuals-quick-guides
Sn500	3-D velocity profiler	Nortek	0.1 cm/s	± 0.5 cm/s	https://www.nortekgroup.com/manuals-quick-guides
MAV	High-resolution single-point 3-D velocity	Nobska	0.03 cm/s 0.1 °	0.3 cm/s ± 2°	http://www.nobska.net/page18/index.html

References

Albrecht, N., Vennell, R., Williams, M.J.M., Stevens, C.L., Langhorne, P.J., Leonard, G., Haskell, T.G., 2006. Observation of sub-inertial internal tides in McMurdo Sound, Antarctica. Geophys. Res. Lett. 33, L24606.

Barrett, P.J., Carter, L., Damiani, C., Dunbar, G.B., Dunker, E., Giorgetti, G., Harper, M.A., McKay, R.M., Niessen, F., Nixdorf, U., Pyne, A.R., Riesselmann, C., Robinson, N., Hollis, C., Strong, P., 2005. Oceanography and Sedimentation beneath the McMurdo Ice Shelf in Windless Bight, Antarctica, Antarctic Data Series 25. 100 pp. Antarctic Research Centre, Wellington, pp. 2005.

Block, B.D., Denfeld, B.A., Stockwell, J.D., Flaim, G., Grossart, H.-P.F., Knoll, L.B., Maier, D.B., North, R.L., Rautio, M., Rusak, J.A., Sadro, S., Weyhenmeyer, G.A., Bramburger, A.J., Branstrator, D.K., Salonen, K., Hampton, S.E., 2019. The unique methodological challenges of winter limnology. Limnol. Oceanogr. Methods 17, 42–57.

Büchner, S., Heuer, A., 2000. Metastable states as a key to the dynamics of supercooled liquids. Phys. Rev. Lett. 84, 2168.

Carstens, T., 1966. Experiments with supercooling and ice formation in flowing water.

Geofysike Publikasjoner 26 (9), 3–18.
Coachman, L.K., Barnes, C.A., 1964. Surface Water in the Eurasian Basin of the Arctic Ocean. Arctic 15 (4), 251–278. https://www.jstor.org/stable/40507022.
Clontz, N.A., McCabe, W.L., 1971. Contact nucleation of $MgSO_4$ $7H_2O$. Chem. Eng. Prog. Symp. Ser. 67, 6–17 No 110.
Craven, M., Warner, R.C., Galton-Fenzi, B.K., Herraiz-Borreguer, L., Vogel, S.W., Allison, I., 2014. Platelet ice attachment to instrument strings beneath the Amery Ice Shelf, East Antarctica. J. Glaciol. 60 (220), 383–393. https://doi.org/10.3189/2014JoG13J082.
Daly, S., 1984. Frazil Ice Dynamics. USA Cold Regions Research and Engineering Laboratory, Monograph 84-1, Hanover, NH.
Daly, S.F., 1991. Frazil Ice Blockage of Intake Trash Racks. USA Cold Regions Research and Engineering Laboratory, Hanover, New Hampshire Technical digest ADA235724.
Daly, S., 2008. Evolution of frazil ice. In: 19th IAHR International Symposium on Ice, "Using technology to understand water-ice interaction", Vancouver, British Columbia, Canada, July 6 to 11, 2008.
Dayton, P.K., Robilliard, G.A., DeVries, A.L., 1969. Anchor ice formation in McMurdo Sound, Antarctica, and its biological effects. Science 163 (3864), 273–274. New Series. http://www.jstor.org/stable/1725104.
Dempsey, D.E., Langhorne, P.J., Robinson, N.J., Williams, M.J.M., Haskell, T.G., Frew, R.D., 2010. Observation and modeling of platelet ice fabric in McMurdo Sound, Antarctica. J. Geophys. Res. 115, C01007. https://doi.org/10.1029/2008JC005264.
Dieckmann, G.S., Rohardt, G., Hellmer, H.H., Kipfstuhl, J., 1986. The occurrence of ice platelets at 250 m depth near the Filchner Ice Shelf and its significance for sea ice biology. Deep Sea Res. A Oceanogr. Res. Pap. 33 (2), 141–148. https://doi.org/10.1016/0198-0149(86)90114-7.
Dorsery, N.E., 1948. The freezing of supercooled water. Trans. Am. Philos. Soc. 38 (3), 245–328.
Drucker, R., Martin, S., Moritz, R., 2003. Observations of ice thickness and frazil ice in the St. Lawrence Island polynya from satellite imagery, upward looking sonar, and salinity/temperature moorings. J. Geophys. Res. 108 (C5), 3149.
Dubé, M., Turcotte, B., Morse, B., 2014. Inner structure of anchor ice and ice dams in steep channels. Cold Reg. Sci. Technol. 106–107, 194–206.
Engelhardt, H., Determann, J., 1987. Borehole evidence for a thick layer of basal ice in the central Ronne Ice Shelf. Nature 327, 318–319.
Feistel, R., 2008. A Gibbs function for seawater thermodynamics for −6 to 80 °C and salinity up to 120 g kg^{-1}. Deep Sea Res. I Oceanogr. Res. Pap. 55, 1639–1671.
Fofonoff, N.P., Millard, R.C., 1983. Algorithms for computation of fundamental properties of seawater. Unesco Technical Papers in Marine Science 44 (4) 53 pp. https://www.jstor.org/stable/40507022.
Foldvik, A., Kvinge, T., 1974. Conditional instability of sea water at the freezing point. Deep-Sea Res. Oceanogr. Abstr. 22, 169–174.
Foldvik, A., Kvinge, T., 1977. Thermohaline convection in the vicinity of an ice shelf. In: Dunbar, M.J. (Ed.), Polar Oceans. Arctic Institute of North America, Calgary, pp. 247–255.
Fricker, H.A., Popov, S., Allison, I., Young, N., 2001. Distribution of marine ice beneath the Amery Ice Shelf. Geophys. Res. Lett. 28, 2241–2244. https://doi.org/10.1029/2000GL012461.
Golovin, K., Kobaku, S.P.R., Lee, D.H., DiLoreto, E.T., Mabry, J.M., Tuteja, A., 2016. Designing durable icephobic surfaces. Sci. Adv. 2 (3). https://doi.org/10.1126/sciadv.1501496. e1501496.
Grosfeld, K., Hellmer, H.H., Jonas, M., Sandhger, H., Schulte, M., Vaughan, D.G., 1998. Marine ice beneath Filchner Ice Shelf: evidence from a multi-disciplinary approach. In: Jacobs, S., Weiss, R. (Eds.), Ocean, Ice and Atmosphere: Interactions at the Antarctic Continental Margin, Antarctic Res. Ser. Vol. 75. AGU, Washington, DC, pp. 319–339.
Hattermann, T., Nøst, O.A., Lilly, J.M., Smedsrud, L.H., 2012. Two years of oceanic observations below the Fimbul Ice Shelf, Antarctica. Geophys. Res. Lett. 39, L12605. https://doi.org/10.1029/2012GL051012.
Hobbs, P.V., 1974. Ice Physics. Oxford University Press, London.
Hodgson, T.V., 1907. On collecting in Antarctic seas. In: British National Antarctic Expedition, 1901–1904, Vol. 3, Zoology and Botany. Trustees of the Brit. Museum, London, pp. 1–10.
Holland, P.R., Feltham, D.L., 2005. Frazil dynamics and precipitation in a water column with depth-dependent supercooling. J. Fluid Mech. 530, 101–124.
Holland, P.R., Corr, H.F.J., Vaughan, D.G., Jenkins, A., Skvarca, P., 2009. Marine ice in Larsen Ice Shelf. Geophys. Res. Lett. 36, L11604. https://doi.org/10.1029/2009GL038162.
Hoppmann, M., et al., 2015. Ice platelets below Weddell Sea land fast sea ice. Ann. Glaciol. 56 (69), 175–190. https://doi.org/10.3189/2015AoG69A678.
Hughes, K.G., Langhorne, P.J., Leonard, G.H., Stevens, C.L., 2014. Extension of an Ice Shelf Water plume model beneath sea ice with application in McMurdo Sound, Antarctica. J. Geophys. Res. Oceans 119, 8662–8687. https://doi.org/10.1002/2013JC009411.
Hunkeler, P.A., Hoppmann, M., Hendricks, S., Kalscheuer, T., Gerdes, R., 2016. A glimpse beneath Antarctic sea ice: Platelet layer volume from multifrequency electromagnetic induction sounding. Geophys. Res. Lett. 43. https://doi.org/10.1002/2015GL065074.
Hunt, B.M., Hoefling, K., Cheng, C.C., 2003. Annual warming episodes in seawater temperatures in McMurdo Sound in relationship to endogenous ice in notothenioid fish. Antarct. Sci. 15 (3), 333–338.
Ito, M., Oshima, K.I., Fukamachi, Y., Simizu, D., Iwamoto, K., Matsumura, Y., Mahoney, A.R., Eicken, H., 2015. Observations of supercooled water and frazil ice formation in an Arctic coastal polynya from moorings and satellite imagery. Ann. Glaciol. 56 (69).
Kim, Philseok, Wong, Tak-Sing, Alvarenga, Jack, Kreder, Michael J., Adorno-Martinez, Wilmer E., Aizenberg, Joanna, 2012. Liquid-Infused Nanostructured Surfaces with Extreme Anti-Ice and Anti-Frost Performance. ACS Nano 6 (8), 6569–6577. https://doi.org/10.1021/nn302310q.
Kirillov, S., Dmitrenko, I., Rysgaard, S., Babb, C., Ehn, J., Bendtsen, J., Boone, W., Barber, D., Geilfus, N., 2018. The inferred formation of a subice platelet layer below the multiyear landfast sea ice in the Wandel Sea (NE Greenland) induced by meltwater drainage. J. Geophys. Res. Oceans 123, 3489–3506.
Kusahara, K., Hasumi, H., 2014. Pathways of basal meltwater from Antarctic ice shelves: a model study. J. Geophys. Res. Oceans 119, 5690–5704.
Langhorne, P.J., et al., 2015. Ice shelf-ocean heat flux: spatial and temporal distribution of platelet ice around coastal Antarctica. Geophys. Res. Lett. 42, 5442–5451. https://doi.org/10.1002/2015GL064508.
Leonard, G.H., Purdie, C.R., Langhorne, P.J., Haskell, T.G., Williams, M.J.M., Frew, R.D., 2006. Observations of platelet ice growth and oceanographic conditions during the winter of 2003 in McMurdo Sound, Antarctica. J. Geophys. Res. 111 (CO4012).
Leonard, G.H., Langhorne, P.J., Williams, M.J.M., Vennell, R., Purdie, C.R., Dempsey, D.E., Haskell, T.G., Frew, R.D., 2011. Evolution of supercooling under coastal Antarctic Sea ice during winter. Antarct. Sci. 23 (4), 399–409.
Lewis, E.L., Lake, R.A., 1971. Sea ice and supercooled water. J. Geophys. Res. 76 (24).
Lewis, E.L., Perkin, R.G., 1983. Supercooling and energy exchange near the Arctic Ocean surface. J. Geophys. Res. 88 (C12).
Lewis, E.L., Perkin, R.G., 1985. The winter oceanography of McMurdo Sound, Antarctica. In: Jacobs, S.S. (Ed.), Oceanology of the Antarctic Continental Shelf, Volume 43 of Antarctic Research Series. American Geophysical Union, Washington, DC, pp. 145–165.
Littlepage, J.L., 1965. Oceanographic investigations in McMurdo Sound, Antarctica. In: Llano, G. (Ed.), Biology of the Antarctic Seas II, Antarct. Res. Ser., Vol. 5. AGU, Washington, DC, pp. 1–37.
Lueck, R.G., Picklo, J.L., 1990. Thermal inertia of conductivity cells: observations with a SeaBird cell. J. Atmos. Ocean. Technol. 7, 756–768.
Mager, S.M., Smith, I.J., Kempema, E.W., Thomson, B.J., Leonard, G.H., 2013. Anchor ice in polar oceans. Prog. Phys. Geogr. 37 (4), 468–483.
Mahoney, A.R., Gough, A.J., Langhorne, P.J., Robinson, N.J., Stevens, C.L., Williams, M.M.J., Haskell, T.G., 2011. The seasonal appearance of ice shelf water in coastal Antarctica and its effect on sea ice growth. J. Geophys. Res. 116, C11032. https://doi.org/10.1029/2011JC007060.
Makkonen, L., Tikanmäki, M., 2018. Modelling frazil and anchor ice on submerged objects. Cold Reg. Sci. Technol. 151, 64–74.
McDougall, T.J., Barker, P.M., 2011. Getting started with TEOS-10 and the Gibbs Seawater (GSW) Oceanographic Toolbox. 28 pp, SCOR/IAPSO WG127, ISBN 978-0-646-55621-5.
McPhee, M.G., Skogseth, R., Nilsen, F., Smedsrud, L.H., 2013. Creation and tidal advection of a cold salinity front in Storfjorden: 2. Supercooling induced by turbulent mixing of cold water. JGR Oceans 118, 3737–3751.
Michel, B., 1963. Theory of formation and deposit of frazil ice. In: Eastern Snow Conference. Proceedings, 20th, pp. 130–149.
Morozov, E.G., Marchenko, A.V., Fomin, Y.V., 2015. Supercooled water near the Glacier front in Spitsbergen. Izv. Atmos. Ocean. Phys. 51, 203. https://doi.org/10.1134/S0001433815020115.
Muller, A., 1978. Frazil ice formation in turbulent flows. In: Iowa Institute of Hydraulic Research, Report No. 214.
Nicholls, K.W., Makinson, K., Østerhus, S., 2004. Circulation and water masses beneath the northern Ronne Ice Shelf, Antarctica. J. Geophys. Res. 109 (C12), C12017.
Omstedt, A., 1985. On supercooling and ice formation in turbulent sea-water. J. Glaciol. 31 (109), 263–271.
Omstedt, A., Svensson, U., 1984. Modeling supercooling and ice formation in a turbulent Ekman boundary layer. J. Geophys. Res. Oceans 89 (C1).
Osterkamp, T.E., 1977. Frazil ice formation: a review. J. Hydraul. Div. 104 (HY9), 1239–1255 ASCE.
Pawlowicz, R., 2013. Key physical variables in the ocean: temperature, salinity, and density. Nat. Educ. Knowl. 4 (4), 13.
Rack, W., Haas, C., Langhorne, P.J., 2013. Airborne thickness and freeboard measurements over the McMurdo Ice Shelf, Antarctica, and implications for ice density. J. Geophys. Res. Oceans 118 (11).
Rees Jones, D.W., Wells, A.J., 2018. Frazil-ice growth rate and dynamics in missed layers and sub-ice shelf plumes. Cryosphere 12, 25–38.
Reimnitz, E., Kempema, E.W., Barnes, P.W., 1987. Anchor ice, seabed freezing and sediment dynamics in shallow Arctic seas. J. Geophys. Res. 92 (C13), 14,671–14,678.
Richard, M., Morse, B., 2008. Multiple frazil ice blockages at a water intake in the St Lawrence River. Cold Reg. Sci. Technol. 53, 131–149.
Robinson, N.J., 2012. Circulation, Mixing and Interactions in the Ocean Near the Ross Ice Shelf. PhD thesis. University of Otago, New Zealand.
Robinson, N.J., Williams, M.J.M., Barrett, P.J., Pyne, A.R., 2010. Observations of flow and ice-ocean interaction beneath the McMurdo Ice Shelf, Antarctica. J. Geophys. Res. 115, C03025.
Robinson, N.J., Williams, M.J.M., Stevens, C.L., Langhorne, P.J., Haskell, T.G., 2014. Evolution of a supercooled Ice Shelf Water plume with an actively growing subice platelet matrix. J. Geophys. Res. Oceans 119, 3425–3446. https://doi.org/10.1002/2013JC009399.
SeaBird Electronics, 2017. Manual: SBE 19plus V2 SeaCAT Profiler CTD. https://www.seabird.com/profiling/sbe-19plus-v2-seacat-profiler-ctd/family-downloads?productCategoryId=54627473770.
Shi, J., Cheng, Y., Jiao, Y., Hou, J., 2011. Supercooled water in austral summer in Prydz Bay, Antarctica. Chin. J. Oceanol. Limnol. 29 (2), 427–437. https://doi.org/10.1007/s00343-010-0011-5.
Skogseth, R., Nilsen, F., Smedsrud, L.H., 2009. Supercooled water in an Arctic polynya: observations and modelling. J. Glaciol. 55 (189), 43–52.

Smith, I.J., Langhorne, P.J., Haskell, T.G., Trodahl, H.J., Frew, R., Vennell, M.R., 2001. Platelet ice and the land-fast ice of McMurdo Sound, Antarctica. Ann. Glaciol. 33, 21–27.

Stigebrandt, A., 1981. On the rate of ice formation in water cooled by a more saline sublayer. Tellus 33, 604–609.

Tweed, F.S., Roberts, M.J., Russell, A.J., 2005. Hydrologic monitoring of supercooled meltwater from Icelandic glaciers. Quat. Sci. Rev. 24, 2308–2318.

Untersteiner, N, Sommerfeld, R., 1964. Supercooled water and the bottom topography of floating ice. Journal of Geophysical Research 69 (6), 1057–1062.

Wang, S.M., Doering, J.C., 2005. Numerical simulation of supercooling processes and frazil ice evolution. J. Hydraul. Eng. 13 (10), 889–897.

Wright, C.S., Priestley, R.E., 1922. British (Terra Nova) Antarctic Expedition 1910–1913: Glaciology. Harrison and Sons, London, UK.

Zhang, W., Brinn, C., Cook, A., Pascual-Marquez, F., 2017. Ice-release and erosion resistant materials for wind turbines. J. Phys. Conf. Ser. 926, 012002.